Final Report

DOE Award # DE-SC0019052

Award title: Surface Chemistry and Reactions for Bimetallic Au Catalysis

Principal investigator: Bruce E. Koel

Date: 06/16/2023; Period covered: 9/15/2018 - 9/14/2022

Au-based catalysts exhibit high catalytic activities and attractive selectivities for a wide range of reactions. They are especially promising in selective oxidation reactions. It is known that the catalytic properties of Au can be significantly enhanced by addition of other metals, but the development of improved Au-based catalysts is hindered by a lack of fundamental understanding of how the catalytic properties of Au can be controlled and tailored. Our major goal in the current grant is to develop a better understanding of the surface chemistry and catalysis of supported Au catalysts and well-defined Au surfaces under controlled conditions. In addition, catalysts with other metals are compared to pure Au and the corresponding Au bimetallic catalysts. We are using an integral experimental-computational approach that synergistically combines multiple techniques: scanning electron microscopy (SEM), transmission electron microscopy (TEM), scanning transmission electron microscopy combined with energy dispersive X-ray analysis (STEM-EDX), in situ Raman spectroscopy, ultraviolet-visible spectroscopy (UV-vis), in situ diffuse reflectance infrared Fourier transform spectroscopy (DRIFTS), in situ infrared reflection-absorption spectroscopy (IRAS) for both single-crystal and supported catalysts, temperature programmed desorption (TPD), reaction kinetics testing in a batch reactor and a continuous flow reactor, and density functional theory (DFT) calculations. Model catalytic systems with well-defined single-crystal surfaces and monodisperse nanoparticles enable us to calibrate our computational models, and the calibrated models, in turn, allow us to interpret experimental results for practical supported catalysts and guide experiment design and the direction of catalyst development.

Identification of a reactive oxygen structure on Au catalysts

A new structure for an atomic oxygen intermediate on Au surfaces was discovered by studying H_2O_2 formation and decomposition (Fig. 1). This discovery will advance the development of improved Au-based catalysts. Reactions of H_2O_2 formation and decomposition were studied because H_2O_2 or OOH surface species are likely intermediates in selective oxidation over Au catalysts. Metal catalysts that are effective in generating H_2O_2 and OOH are also effective in decomposing these species to form water, resulting in low selectivities. It is therefore, important to better understand at a molecular level the structure and reactivity of H_2O_2, OOH, and oxygen species on Au catalytic surfaces under reaction conditions. A series of SiO_2-supported Au catalysts with different metal loadings and particle sizes were used to carry out liquid-phase H_2O_2 decomposition under multiple reaction conditions. Fundamental composition-structure-activity relationships for Au catalysts were established for H_2O_2 decomposition to H_2O and O_2. Due to the high structure sensitivity of Au catalysts, adsorption and reactivity of reactants, products, and intermediates, along with catalytic reaction rates, were studied using monodisperse 5, 50, and 400-nm Au nanoparticles supported on SiO_2. In situ surface-enhanced Raman spectroscopy (SERS) measurements were performed to identify surface structures and species in the catalytic decomposition of H_2O_2. DFT calculations with vibrational analyses were employed to interpret the Raman spectra and to identify the experimentally observed oxygen structures.

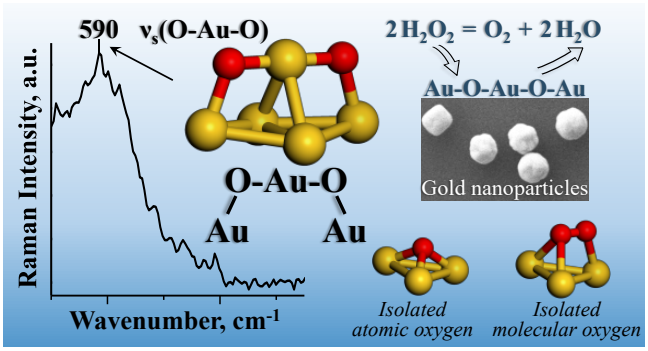

Figure 1. Our study with kinetic measurements, in situ Raman spectroscopic measurements with ^{18}O isotope, and DFT calculations identified a new O-Au-O reaction intermediate during H_2O_2 decomposition on Au catalytic nanoparticles.

Measurements of the kinetics of H_2O_2 decomposition to form gas-phase O_2 and liquid H_2O were performed in a glass Raman cell that served as a batch reactor. The number of Au nanoparticles deposited per unit SiO_2 surface area was adjusted in such a way that the ratio of the surface areas for Au nanoparticles and the SiO_2 support remained constant at 0.13 m^2 Au/m^2 SiO_2. Therefore, the total Au surface area was constant in all experiments. Raman spectroscopy confirmed that the thermal treatment produced spectroscopically clean Au surfaces without organic ligands. The characteristic Raman bands for the ligands at 1299, 1392 and 1545 cm^{-1} were no longer observed after the treatment.

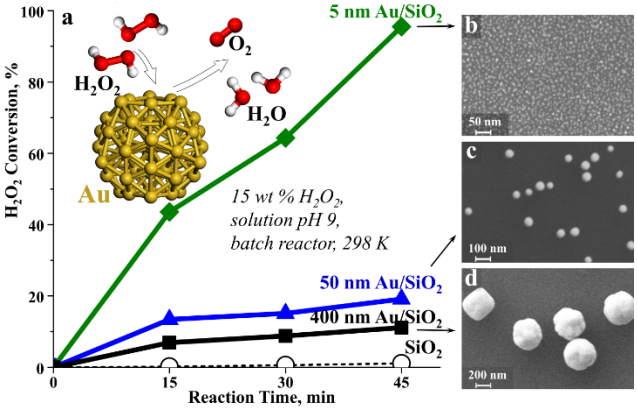

Figure 2. Kinetic measurements with monodisperse 5, 50, and 400-nm Au nanoparticles with the same total Au surface area of 0.13 m^2 Au/m^2 SiO_2 showed that H_2O_2 decomposition with an O-Au-O reaction intermediate is a highly structure-sensitive reaction.

Catalytic decomposition of a 15 wt% aqueous H_2O_2 solution over clean Au catalysts was monitored utilizing in situ SERS measurements for evaluating the time-dependent H_2O_2 conversion (Fig. 2). The spectra were collected as a function of reaction time in a batch reactor at room temperature and pH = 9 for SiO_2-supported Au particles. The reaction rate of H_2O_2 decomposition decreased with increasing Au particle size. The 5-nm Au particles were more catalytically active than the 50 and 400-nm Au particles. After 45 min of reaction time, all H_2O_2 was decomposed over the 5-nm Au catalyst, whereas the H_2O_2 conversion was only 19% and 11% for the 50 and 400-nm Au catalysts, respectively. A blank experiment conducted in the absence of Au showed that the rate of H_2O_2 decomposition was lower over the SiO_2 support alone, with a conversion of less than 1% after 45 min of reaction time. This result confirmed that Au served as a catalyst for H_2O_2 decomposition.

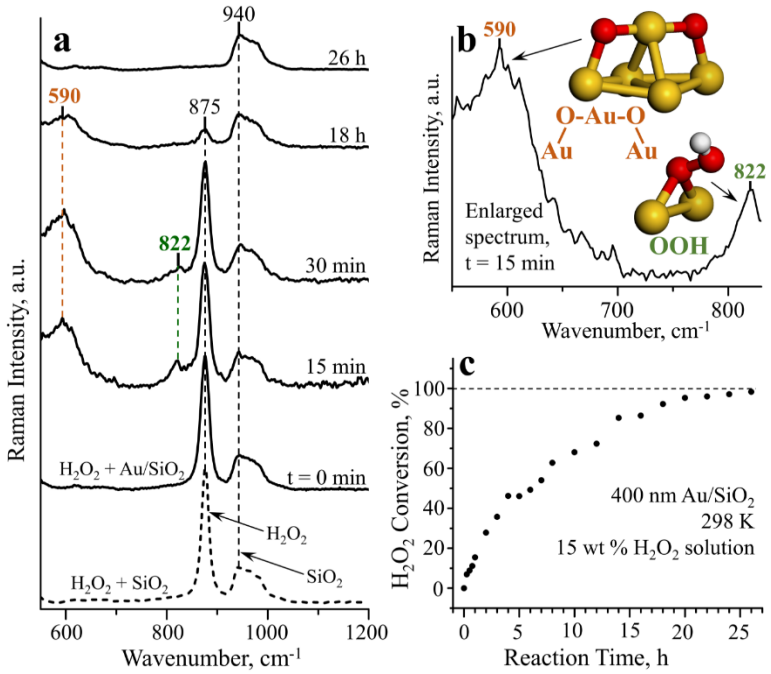

Figure 3. H_2O_2 decomposition over 400-nm Au/SiO_2. **(a)** Evolution of in situ Raman spectra as a function of reaction time plus a comparative spectrum for H_2O_2 over SiO_2 showed the presence of reaction intermediates with bands at 590 and 822 cm^{-1}. **(b)** An enlarged part of the spectrum at 15 min with assignments for the observed reaction intermediates: Au-O-Au-O-Au structure and OOH surface species. **(c)** Dependence of H_2O_2 conversion on reaction time. Raman band assignments were made using DFT calculations: 590 cm^{-1} – Au-O-Au reaction intermediate, 822 cm^{-1} – Au-OOH reaction intermediate, and 875 cm^{-1} – Au-H_2O_2 and liquid-phase H_2O_2.

The time evolution of in situ Raman spectra for the 400-nm Au/SiO_2 catalyst at pH = 9 was compared to a spectrum of the aqueous H_2O_2 solution collected in an experiment without Au under the same conditions (Fig. 3). In addition to the Raman band at 940 cm^{-1} for SiO_2, liquid phase H_2O_2 exhibited a band at 875 cm^{-1}. Immediately after adding H_2O_2 to the 400-nm Au/SiO_2 catalyst (reaction time of zero), essentially the same spectrum with bands at 857 and 940 cm^{-1} was

observed.

After H_2O_2 started to decompose (15 and 30 min of reaction time), two new Raman bands at 590 and 822 cm^{-1} were observed. The intensities of these new bands and the band at 875 cm^{-1} for liquid-phase H_2O_2 remained constant at low H_2O_2 conversion from decomposition. The conversion was 7% after 15 min and 9% after 30 min. After 18 h, when most of the H_2O_2 had decomposed (92% conversion), the bands at 590 and 875 cm^{-1} became smaller and the band at 822 cm^{-1} was no longer observed. When all H_2O_2 decomposed after 26 h (100% conversion), bands at 590 and 875 cm^{-1} were no longer observed, leaving a single band at 940 cm^{-1} from the SiO_2 support. Since the bands at 590 and 822 cm^{-1} were only observed during H_2O_2 decomposition, they must be due to reaction intermediates.

DFT calculations were utilized to identify structures formed by atomic oxygen adsorption on Au surfaces. Two structures described by other experimental and computational studies were identified. The first structure involved isolated O atoms binding on the Au surface at low surface oxygen coverage. The second structure was observed at higher coverage when two oxygen atoms push a neighboring Au atom from the surface into the adlayer to form a dimer denoted as Au_2-O-Au-O-Au_2, with the O atoms in pseudo-threefold sites. In a recent result, we identify a new third structure found on the surface of Au nanoparticles. When O atoms do not need to displace an Au atom from a flat surface, an Au-O-Au-O-Au structure is formed with the O atoms in bridge sites.

DFT calculations were used to assign the in situ Raman band at 822 cm^{-1} to OOH surface species in H_2O_2 decomposition over a 400-nm Au/SiO_2 catalyst. These calculations show that OOH adsorbs preferentially on an Au-Au bridge site with ν(O-O) modes in the range from 831 cm^{-1} for small Au clusters to 806 cm^{-1} for Au(111).

To assign the band at 590 cm^{-1} observed during in situ Raman spectroscopy of H_2O_2 decomposition over a 400-nm Au/SiO_2 catalyst, different possible binding configurations for atomic oxygen were evaluated. The ν(O-Au) modes for isolated O adatoms at three-fold and two-fold bridge sites on Au surfaces were calculated to be 373-467 cm^{-1}. The ν(O-Au-O) mode for the dimer structure denoted as Au_2-O-Au-O-Au_2 was calculated to be 450-508 cm^{-1}, and so also too low to agree with the experiment. However, for the newly identified Au-O-Au-O-Au structure the calculated ν_s(O-Au-O) frequencies were 546-558 cm^{-1}, which is in fairly good agreement with the band at 590 cm^{-1} seen experimentally. Our results obtained during our initial proposal preparation were published in *Angewandte Chemie*[1], and our extended results under this grant were presented by one of the PI's, graduate students and postdocs at several conferences.[2,3,4] One additional manuscript is in preparation.

Identification of catalytically active oxygen species on Ag catalysts

The study of oxygen species on Au catalysts was extended to Ag because Au-Ag is promising as a bimetallic catalyst that is studied for multiple selective hydrocarbon oxidation reactions and since Ag-based catalysts are used industrially with gas-phase oxygen for selective oxidation of ethylene epoxidation to ethylene oxide and methanol oxidation to formaldehyde. Furthermore, interactions of oxygen with Ag are investigated in multiple areas of science and technology, including materials science, medical and biomedical applications, physics, spectroscopy and photonics, and for designing plasmon-mediated chemical reactions, including effective solar-to-chemical energy conversion.

Gas-phase O_2 adsorbs on Ag molecularly by preserving the O-O bond and atomically by breaking the O-O bond. Molecular adsorbed O_2 structures have O-O vibrational frequencies at 860-1150 cm^{-1}. Atomic adsorbed O structures have Ag-O vibrational frequencies at 240-500 cm^{-1}. In our study, we for the first time identify hybrid atomic-molecular oxygen structures on Ag surfaces using Raman spectroscopic measurements and density functional theory calculations (Fig. 4). These hybrid O-O structures form when one adsorbed O atom reacts with one lattice O atom on the surface or in the subsurface of Ag. These hybrid O-O structures do not form by a recombination of two adsorbed O atoms because one of the O atoms in the

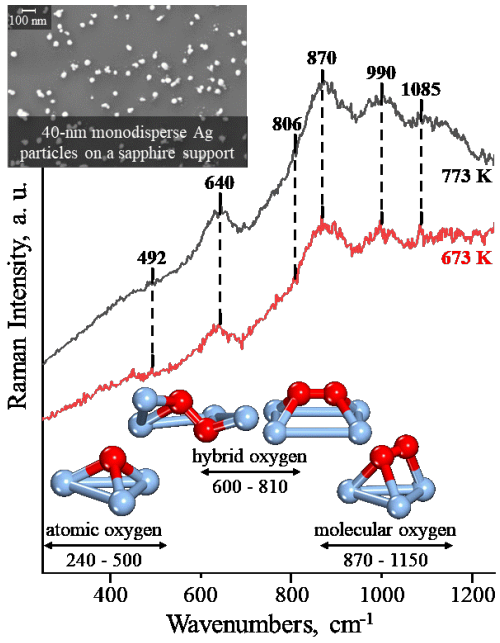

Figure 4. Our in situ Raman measurements and DFT calculations identified an oxygen reaction intermediate on Ag nanoparticles. The intermediate is a hybrid between atomic-molecular oxygen structures formed when one adsorbed O atom reacts with one lattice O atom in the Ag subsurface.

hybrid structure must be embedded in the Ag lattice. In contrast with molecular adsorbed O_2 structures, the hybrid structures have O-O vibrational frequencies of 600-840 cm^{-1}. Furthermore, the hybrid structures are metastable on metallic, partially oxidized, and oxidized Ag surfaces and therefore, serve as highly active reaction intermediates in catalytic selective oxidation reactions. A graduate student presented the results at a conference.[5] The study was published in *Langmuir* in 2021.[6] An extended abstract entitled "Identification of Catalytically Active Oxygen Structures on Silver" was submitted for presentation at NAM-27.[7]

Structure-insensitivity of OH groups on Au catalytic surfaces

Our study using in situ diffuse reflectance infrared Fourier transform spectroscopy (DRIFTS) measurements and DFT calculations for a series of Au catalysts supported on ZSM-5 zeolites for the first time demonstrated that in contrast to the structure and reactivity of H_2O_2, OOH, O_2, and O that are highly dependent on the size of Au nanoparticles, the structure and reactivity of OH is structure-insensitive as it remains the same on Au particles of different sizes and on bulk Au surfaces. Furthermore, preferential anchoring sites for Au nanoparticles on zeolites were identified as framework Al sites.

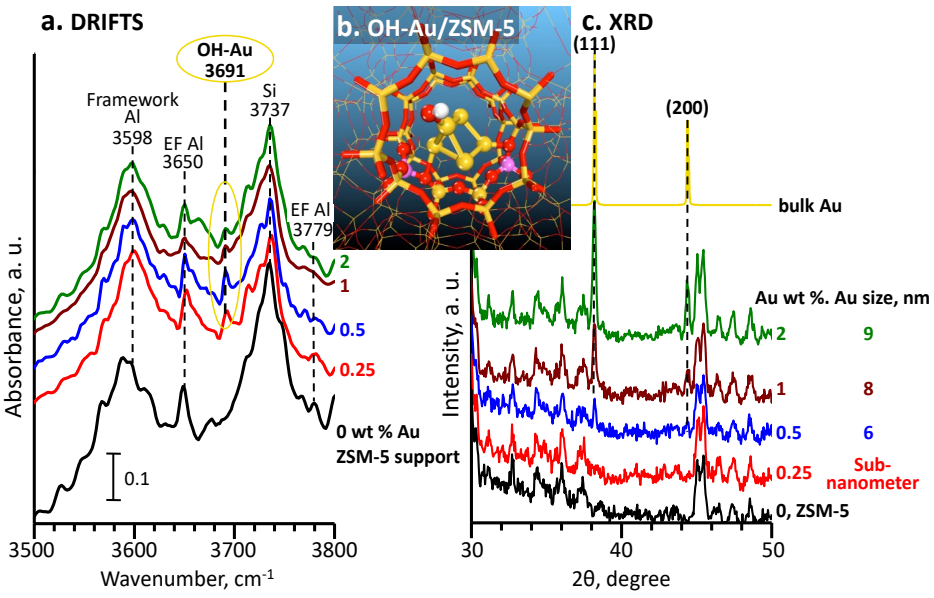

Figure 5. Our in situ DRIFTS measurements for Au/ZSM-5 catalysts provide the first direct experimental observation of OH on Au nanoparticles. The catalysts were tested in ethanol oxidation to acetic acid. Our DFT calculations show that in contrast with adsorbed O, O_2, and OOH, which are highly sensitive to the size of Au particles, the structure of OH remains the same on Au particles of different sizes and on bulk Au surfaces.

Four IR peaks for the OH vibrations were observed for ZSM-5 and correspond to different types of surface OH groups (Fig. 5a). A peak at 3598 cm^{-1} was assigned to vibrations of Brønsted acid hydroxyls on zeolite framework Al sites. A peak at 3737 cm^{-1} was due to vibrations of Si-OH groups on the external surface of the zeolite. Peaks at 3650 and 3779 cm^{-1} were assigned to the OH groups on extraframework Al sites. A new peak at 3691 cm^{-1} was assigned to OH species on Au nanoparticles (Fig. 5b). This is the first direct

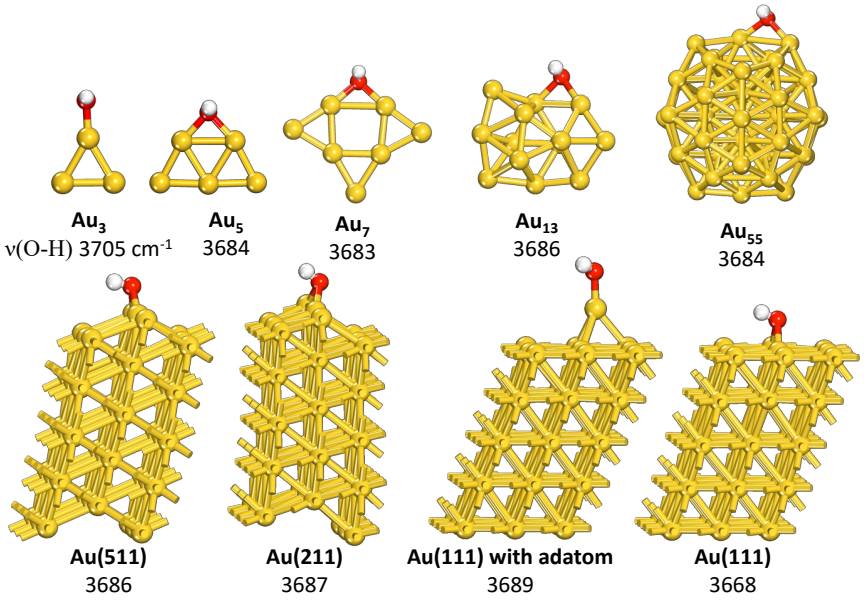

Figure 6. Geometries of hydroxyls on Au surfaces ranging from Au_3-Au_{13} clusters, to a Au_{55} particle with a size of ~1 nm and to periodic bulk Au surfaces obtained with our DFT calculations. The listed numbers are calculated O-H bond stretching vibrational frequencies, ν(O-H), cm^{-1}.

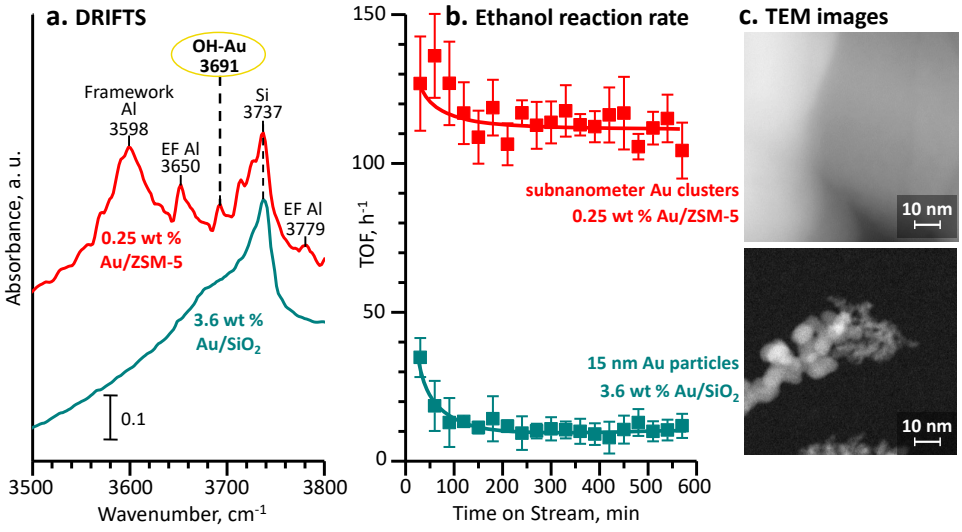

Figure 7. (a) DRIFTS spectra, **(b)** ethanol reaction rates in selective oxidation with gas-phase oxygen in a flow reactor at 333 K and atmospheric pressure, and **(c)** TEM images for 0.25 wt % Au/ZSM-5 and 3.6 wt % Au/SiO_2. These catalysts had the same number of surface Au atoms. These results demonstrate that the O-H stretching vibration for hydroxyls on Au can serve as a qualitative indicator of the roughness of the Au surface and functional properties associated with the presence of coordinatively unsaturated surface gold atoms, such as catalytic activity.

experimental observation of OH species on Au nanoparticles. Our DFT calculations for Au particles with sizes in a wide range, from small clusters to large nanoparticles, as well as Au crystal planes, demonstrate that the structure of OH on all Au surfaces is the same with the same vibrational frequency for the O-H stretching vibration, explaining the experimental observations (Fig. 6). In catalytic selective oxidation of ethanol with gas-phase oxygen, the reaction activity of subnanometer Au particles, for which hydroxyls were observed at 3694 cm^{-1}, was 10 times higher than that of 15-nm Au particles, for which hydroxyls were not observed, when the total number of surface gold atoms for both catalysts was the same (Fig. 7). The results were submitted as a joint publication entitled "Observation and Structure-Insensitivity of Hydroxyls on Gold" by Koel and Podkolzin to *JACS* in 2021.[8] An extended abstract with the same title was submitted for presentation at NAM-27.[9]

Ethanol selective oxidation

Selective oxidation of alcohols to aldehydes and acids is important in the production of numerous value-added chemicals. Ethanol is often used as a model compound in the development of new selective oxidation processes. Furthermore, ethanol can be produced from biomass and, therefore is a sustainable feedstock for commodity and specialty chemicals. Ethanol oxidation is currently performed using chromate or permanganate

compounds, which are hazardous and expensive. Therefore, it is desirable to develop new environmentally friendly catalysts that can use inexpensive gas-phase oxygen or air as the oxidant.

In this study, a series of zeolite-supported gold catalysts were synthesized, characterized and tested in a fixed-bed flow reactor for ethanol selective oxidation. The catalysts exhibited high activities and selectivities at mild reaction conditions. Effects of the Au loading, morphology of the support, and zeolite Si/Al ratio were evaluated. TEM and in situ DRIFTS as well as DFT calculations were used to provide molecular-level understanding of the nature of active sites and the reaction mechanism.

Two sets of Au/ZSM-5 catalysts were synthesized. In the first set, the Au loading was constant at 1 wt%, while the Si/Al ratio of the ZSM-5 support varied from 15 to 140. In the second set, the Si/Al ratio was constant at 15, while the Au loading varied from 0.25 to 2 wt%. The catalysts were tested in a packed-bed flow reactor. The catalysts were dried in situ prior to reaction testing and then tested without reduction for ethanol oxidation. During the reaction, a gas feed of 30 mol% O_2/He with a total flow rate of 100 sccm was used. A 0.02 ml/min flow of liquid ethanol was fed and mixed as vapor with the gas flow in a preheater. The ethanol flow rate was selected to ensure that the partial pressure of ethanol was lower than its saturation pressure. Reaction products were analyzed with an online gas chromatograph equipped with a thermal conductivity detector and a flame ionization detector. Additional supports, SiO_2 and S-1, were compared to ZSM-5 to evaluate acidity and morphology effects of the support.

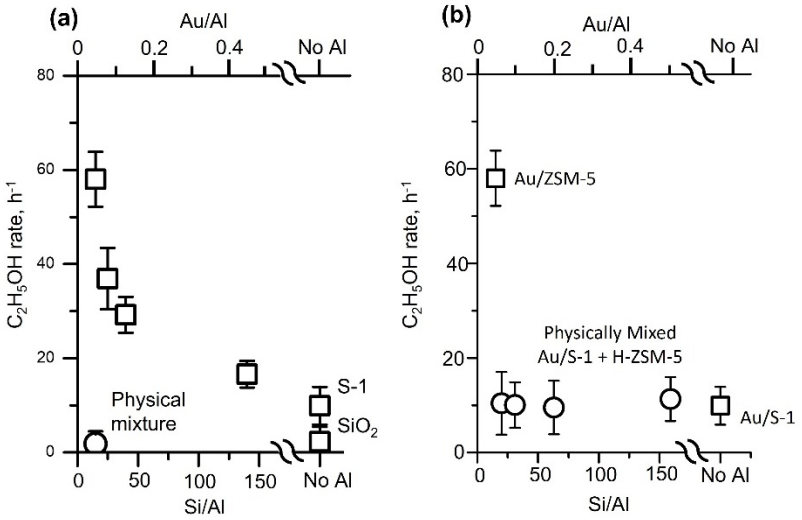

Figure 8. Ethanol oxidation rate effects of Si/Al ratios for **(a)** 1 wt % Au/ZSM-5 (Si/Al=15-140 plus S-1), 1 wt % Au/SiO_2 is shown for comparison, and **(b)** physical mixtures of 1 wt % Au/S-1 and ZSM-5 (Si/Al=15) without Au (□ - catalysts prepared by incipient wetness impregnation of Au, ○ – physical mixtures). 333 K, atmospheric pressure.

The main products in gas-phase ethanol selective oxidation with O_2 at 333 K were acetaldehyde (69-89 mol%) and acetic acid (11-30 mol%). Importantly, overoxidation to CO and CO_2 were completely suppressed. The ethanol reaction rate at 333 K increased by a factor of 3 when 1 wt% Au was deposited on S-1 silicalite compared to the same Au loading on an amorphous SiO_2 support. This effect was attributed to a better dispersion of Au particles on the MFI structure of S-1 based on TEM and XRD measurements. When the same 1 wt % Au was deposited on ZSM-5 (Si/Al=15, the same MFI structure), the reaction rate increased to 58 mol ethanol/mol of Au/h, by a factor of 26 higher than that for 1 wt % Au/SiO_2 (Fig. 8). The presence of Al sites in the MFI structure, thus, dramatically increased the catalytic activity. Moreover, the catalytic activity declined with decreasing concentration of framework Al sites (higher Si/Al ratios in Fig. 8a). This effect can be due to either the activity of Al sites by themselves or synergy between Al and Au sites. Reaction testing results of physical mixtures with different ratios of 1 wt % Au/S-1 and ZSM-5 (Si/Al=15) without Au in Fig. 8b demonstrate that the mere presence of zeolite Al sites does not change the reaction rate. Therefore, the Al sites are not active by themselves, and the synergistic effect requires proximity of Au and Al sites. In addition to the increased activity, 1 wt % Au/ZSM-5 exhibited better stability than the SiO_2-supported catalyst. The participating postdoc presented the results at a local meeting of the Catalysis Society of Metropolitan New York and at the national ACS meeting.[10,11] One manuscript is in preparation. An extended abstract entitled "Selective Oxidation of Ethanol over Zeolite-Supported Gold Catalysts" was submitted for presentation at NAM-27.[12]

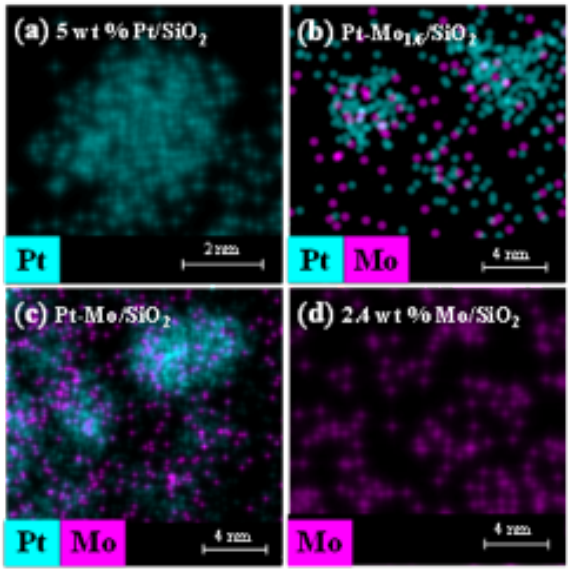

Figure 9. Microscopy images of SiO_2-supported **(a)** Pt, **(b)** Pt-$Mo_{1/6}$, **(c)** Pt-Mo and **(d)** Mo catalysts. The STEM-EDX images show Pt particles with an average size of 3.2 nm that are mostly unaffected by the presence of Mo. Mo forms sub-nm clusters that are fairly uniformly distributed on the surface, with or without Pt. For Pt-Mo catalysts, Pt nanoparticles are decorated with Mo clusters. With increasing Mo concentration, the number of Mo clusters increases while their size remains mostly the same.

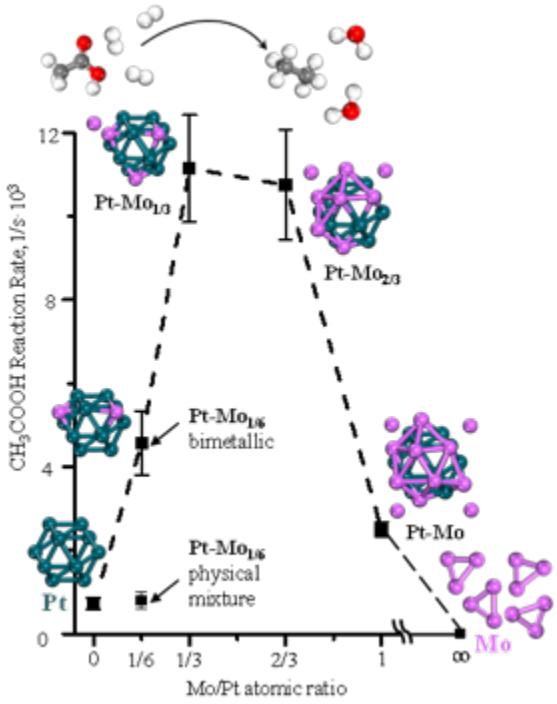

Figure 10. Effect of Mo addition to Pt on catalyst activity in gas-phase acetic acid hydrodeoxygenation in a flow reactor. 0.1 g of catalyst, 40 mol % H_2/N_2 with a total flow rate of 100 sccm, 0.03 ml/min liquid acetic acid, 423 K, 1 atm. Pt, Mo and Pt-Mo nanoparticles were supported on SiO_2. The Pt concentration was kept constant at 5 wt %, the Mo concentration was varied. The monometallic 5 wt % Pt/SiO_2 catalyst and the physical mixture of monometallic Pt and Mo catalysts with a Mo/Pt ratio of 1/6 had low activities. The monometallic 2.4 and 0.4 wt % Mo/SiO_2 catalysts were inactive. The bimetallic Pt-Mo catalysts exhibited high activities with a maximum at a Mo/Pt ratio of 1/3.

Acetic acid hydrodeoxygenation over Pt and Pt-Mo catalysts

As a reference for future studies of Au-Pt, Au-Mo and Au-Pt-Mo catalysts, Pt-Mo bimetallic catalysts were studied with TEM, STEM-EDX (Fig. 9), X-ray absorption near edge structure (XANES), extended X-ray absorption fine structure (EXAFS), kinetic measurements in a fixed-bed flow reactor, and DFT calculations. The results demonstrate that Pt nanoparticles decorated with subnanometer Mo clusters can efficiently catalyze hydrodeoxygenation of acetic acid, which serves as a model biomass compound. In contrast with monometallic Mo catalysts that are inactive and monometallic Pt catalysts that have low activities and selectivities, bimetallic Pt-Mo catalysts exhibited synergistic effects producing high activities and selectivities. The maximum activity occurred at a Mo:Pt molar ratio of $^1/_3$ (Fig. 10). Although Mo atoms themselves are catalytically inactive, they serve as preferential binding anchors for oxygen atoms while a catalytic transformation proceeds on neighboring surface Pt atoms. Initial results were published in *Chemistry – A European Journal*.[13] One of the PI's presented the extended results under this grant at a conference.[14] An additional publication entitled "Kinetics and Reaction Mechanisms of Acetic Acid Hydrodeoxygenation over Pt and Pt-Mo Catalysts" is in revisions at *ACS Sustainable Chemistry & Engineering*.[15] The manuscript is a collaboration with scientists at BIOVIA Corporation, Dr. Felix Hanke and Dr. Victor Milman in Cambridge, UK, on the development of better DFT codes in the description of hydrocarbon reactivity on surfaces of transition metal catalysts. One additional manuscript in collaboration with Dr. Jeffrey T. Miller at Purdue University is in preparation.

Acetic acid adsorption and reactions on Ni and Pt catalysts

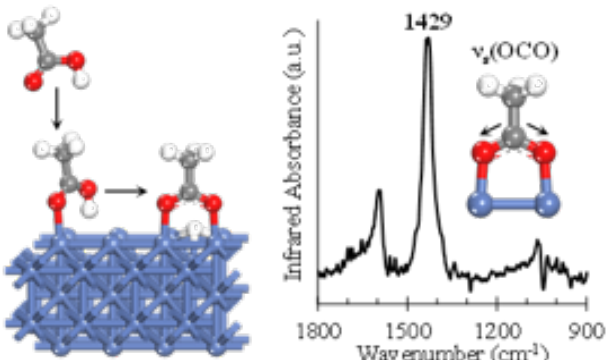

Figure 11. Our study with TPD and in situ IRAS measurements as well as DFT calculations determined adsorption structures and reactivity of acetic acid on Ni(110). The dominant IR peak at 1429 cm^{-1} is due to a bidentate acetate structure.

As a reference for studying Au-Ni and Au-Pt bimetallic catalysts, Ni and Pt single crystal surfaces as well as supported catalysts were studied. Adsorption and surface reactions of acetic acid at multiple surface coverages on Ni(110) and Pt(111) was studied with TPD and IRAS at 90-500 K. In addition, acetic acid hydrodeoxygenation over Pt/SiO_2 and Ni/SiO_2 powder catalysts was evaluated in a packed bed flow reactor. Acetic acid adsorbed mostly molecularly below the monolayer saturation coverage of 0.36 ML on Ni (110) at 90 K. Above this coverage, two physisorbed multilayer desorption peaks were observed at 157 and 172 K, which were assigned to the decomposition of dimers and catemers, respectively. Between 90 and 200 K, the Ni surface breaks the O-H bond in acetic acid and forms acetate species. The bidentate acetate had a characteristic ν_s(OCO) vibration at 1421-1429 cm^{-1} (Fig. 11). Minor species at 200 K were identified as acetyl species with a ν(C=O) vibration at 1595-1690 cm^{-1}. Concurrent desorption of H_2, CO, and CO_2 at 425 K demonstrated that the surface acetate species and all other remaining hydrocarbon species decomposed simultaneously at this temperature. The results were published in *Langmuir*.[16]

Similar results were obtained on Pt(111). At 90 K, acetic acid formed a physisorbed layer on Pt(111). At 140 K, acetic acid predominantly chemisorbed molecularly through the carbonyl oxygen atom. In addition, some dissociative adsorption was observed with the formation of acetate and hydrogen. Annealing to 193 K led to a mostly complete conversion of molecularly adsorbed acetic acid to acetate species. At 440 K, acetate species decomposed, evidenced by desorption of H_2, CO, and CO_2. Despite similarities in acetic acid adsorption on Ni and Pt crystals in ultrahigh vacuum surface science studies, Ni and Pt catalytic activities in supported catalysts were dramatically different. Pt was significantly more active and selective in producing C_2 hydrocarbons. This catalytic performance difference was attributed to the formation of a surface oxide layer on Ni, which requires higher reduction temperatures in the catalytic cycle. A graduate student presented the results at a conference.[17] One additional manuscript is in preparation. An extended abstract entitled "Acetic Acid Adsorption and Reactions on Pt and Ni" was submitted for presentation at NAM-27.[18]

Furfural adsorption on Pt

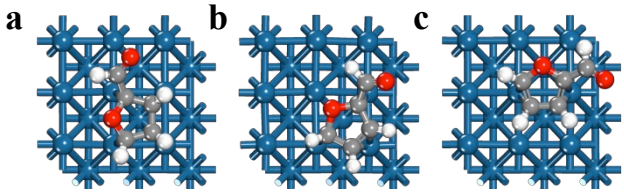

Figure 12. Preferential furfural adsorption structures on Pt(100) identified with DFT calculations: **(a)** fourfold site, **(b)** threefold site, and **(c)** bridge site.

Furfural (2-furancarboxaldehyde) is one of the major components of bio-oils, and it has been widely used as a model compound in the development of more efficient technologies for biomass conversion into fuels and chemicals feedstocks. Although Pt-based catalysts have been studied as promising catalysts for hydrodeoxygenation of bio-oils and other upgrading technologies, the fundamentals of furfural adsorption and reactions on Pt surfaces at the molecular level are still not well understood. In this study, furfural adsorption on a Pt(100) surface was studied with IRAS and TPD measurements at different surface coverages in a wide temperature range. In addition, DFT calculations were used to determine geometries, adsorption energies, and vibrational frequencies for adsorption structures (Fig. 12). A graduate student presented the results at a conference.[19] One manuscript is in preparation. An extended abstract entitled "Furfural Adsorption and Reactivity on Platinum Catalysts" was submitted for presentation at NAM-27.[20]

Propane dehydrogenation to propylene over Ni and Ni-Sn catalysts

To satisfy the growing demand for olefins, catalytic dehydrogenation of paraffins can be used. In this work, the fundamentals of propylene adsorption and reactivity were studied on Ni and Ni-Sn, which are promising catalysts for propane dehydrogenation to propylene. Experimental measurements using TPD and IRAS were combined with DFT calculations. A Ni(110) single crystal surface was compared with a Sn/Ni(110) surface alloy that had a c(2×2) structure with a Ni:Sn atomic ratio of unity (Fig. 13). DFT calculations with vibrational analyses identified adsorption structures by matching the experimental IR spectra. Propylene preferentially adsorbs on pure Ni in a di-σ and π bonding configuration. In contrast, the presence of Sn forces propylene to adsorb in a less stable π-bonded configuration. Furthermore, on the Ni-Sn surface propylene decomposition with the formation of surface propylidyne and hydrogen species becomes thermodynamically unfavorable, and this reaction is completely suppressed. In addition, reaction measurements in a flow reactor were performed with Ni/SiO_2 and $Ni-Sn/SiO_2$ catalysts in a packed bed flow reactor. A graduate student presented the results at a conference.[21] Manuscript entitled "Propane Dehydrogenation to Propylene and Propylene Adsorption on Ni and Ni-Sn Catalysts" is in revisions at *ChemCatChem*.[22] An extended abstract entitled "Propane Dehydrogenation to Propylene on Ni and Ni-Sn Catalysts" was submitted for presentation at NAM-27.[23]

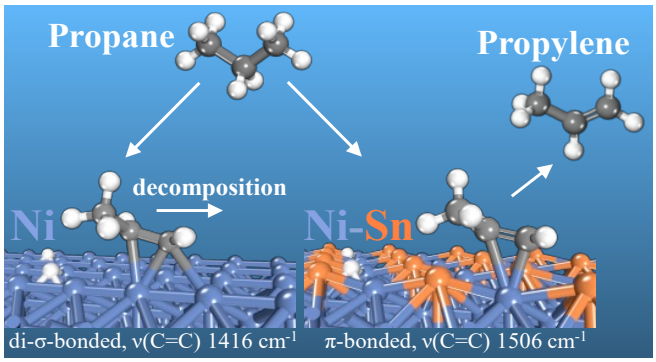

Figure 13. Our DFT calculations determined structures, adsorption energies, and vibrational frequencies for propylene on Ni and Ni-Sn surfaces. The calculations explained our experimental TPD and in situ IRAS results. The presence of Sn completely suppressed propylidyne formation and C-C bond breaking, significantly enhancing the selectivity in propane dehydrogenation to propylene.

Propylene epoxidation over Au-Pt and Au-Pd catalysts

Propylene oxide is an important commodity chemical used in the production of polyurethane and polyols. It is highly desirable to develop a single-step process for propylene epoxidation using gas-phase O_2. Our results show that TiO_2-supported Au-Pt and Au-Pd catalysts exhibit better performances for propylene epoxidation with O_2 in the presence of H_2 than the corresponding monometallic Au, Pt, and Pd catalysts. The Au loading for the monometallic catalyst was 0.5 wt %. The Pt and Pd loadings were 0.5 and 0.27 wt % to match the atomic Au loading. The Au to Pt and Pd ratio in the bimetallics was varied in a wide range, from 20:1 to 1:20. Propylene conversion over Au/TiO_2 was low (0.9%) with low selectivity (5%) due to the formation of undesirable C_3 products and over-oxidation products (ethanol and CO_2). Monometallic Pt and Pd catalysts were very active with higher than 97% conversion but with practically zero selectivity: no propylene oxide was detected. In contrast, Au-rich bimetallics were both active and selective. TEM experiments are ongoing to better understand the structure of the Au bimetallics and guide the development of improved catalysts. One manuscript is in preparation.

List of publications

Intellectually driven by the DOE award (can be exclusively funded by the grant or jointly funded with leading intellectual contribution from the DOE grant)

- Yiteng Zheng, Yue Qi, Ziyu Tang, Jun Zhi Tan, Simon G. Podkolzin, Bruce E. Koel, "Spectroscopic Observation and Structure-Insensitivity of Hydroxyls on Gold". *ChemComm.*, 58, 4036-4039 (2022). DOI:10.1039/D2CC00283Cq.
- Jason P. Robbins, Lotanna Ezeonu, Ziyu Tang, Xiaofang Yang, Simon G. Podkolzin, Bruce E. Koel, "Propane Dehydrogenation to Propylene and Propylene Adsorption on Ni and Ni-Sn Catalysts". *ChemCatChem,* 14(6), e202101546 (1 of 12) 2022. DOI:10.1002/cctc.202101546

- Ziyu Tang, Tao Chen, Kai Liu, Henry Du, Simon G. Podkolzin, "Atomic, Molecular and Hybrid Oxygen Structures on Silver". *Langmuir* **2021**, 37 (39), 11603-11610. DOI: 10.1021/acs.langmuir.1c01941.
- Yiteng Zheng, Yue Qi, Ziyu Tang, Felix Hanke, Victor Milman, Simon G. Podkolzin, "Kinetics and Reaction Mechanisms of Acetic Acid Hydrodeoxygenation over Pt and Pt-Mo Catalysts". *ACS Sustainable Chemistry & Engineering* **2021**, submitted manuscript sc-2021-07639c.
- Michelle S. Hofman, Emanuel V. Scoullos, Jason P. Robbins, Lotanna Ezeonu, Denis V. Potapenko, Xiaofang Yang, Simon G. Podkolzin, Bruce E. Koel, "Acetic Acid Adsorption and Reactions on Ni(110)", *Langmuir* **2020**, 36 (30), 8705–8715. DOI: 10.1021/acs.langmuir.0c00713.
- Jason P. Robbins, Kai Liu, Fei Tian, Simon G. Podkolzin, "Hydrogen Peroxide Decomposition over Monodisperse Spectroscopically Clean Gold Nanoparticles", manuscript in preparation.
- Ziyu Tang, Tao Chen, Kai Liu, Simon G. Podkolzin, "Structures and Vibrational Frequencies of Oxygen on Silver", manuscript in preparation.
- Yiteng Zheng, Bruce E. Koel, Simon G. Podkolzin, "Selective Oxidation of Ethanol over Zeolite-Supported Gold Catalysts", manuscript in preparation.
- Yiteng Zheng, Ziyu Tang, Stephen C. Purdy, Jeffrey T. Miller, Simon G. Podkolzin, "Surface and Bulk Structures of Pt-Mo Catalysts", manuscript in preparation.
- Lotanna Ezeonu, Jason P. Robbins, Xiaofang Yang, Bruce E. Koel, Simon G. Podkolzin, "Acetic Acid Adsorption and Reactions on Pt and Ni Catalysts", manuscript in preparation.
- Yue Qi, Emanuel V. Scoullos, Yiteng Zheng, Bruce E. Koel, Simon G. Podkolzin, "Adsorption and Reactivity of Furfural on Platinum", manuscript in preparation.
- Yiteng Zheng, Simon G. Podkolzin, Bruce E. Koel, "Propylene Epoxidation over Au-Pt and Au-Pd Catalysts", manuscript in preparation.

The project results were presented in 20 conference presentations by the PIs, postdocs, and graduate students, including invited talks and prominent international conferences, such as ACS National Meetings, NAM-26 and NAM-27.[2-5, 7, 9-12, 14, 17-21. 23-27]

Jointly funded by the DOE award and other grants, but not intellectually driven by the DOE grant. None to report.

References

1. Liu, K.; Chen, T.; He, S.; Robbins, J. P.; Podkolzin, S. G.; Tian, F., Observation and Identification of an Atomic Oxygen Structure on Catalytic Gold Nanoparticles. *Angewandte Chemie International Edition* **2017**, *56* (42), 12952-12957.

2. Liu, K.; Chen, T.; He, S.; Robbins, J.; Tian, F.; Podkolzin, S. G. In *Observation and Identification of an Atomic Oxygen Structure on Gold in Catalytic Decomposition of Hydrogen Peroxide*, 26th North American Catalysis Society Meeting(NAM26), Chicago, IL, 2019.

3. J.P. Robbins; K. Liu; T. Chen; S. He; F. Tian; Podkolzin, S. G. In *Kinetic, Spectroscopic and Computational Study of Hydrogen Peroxide Decomposition over Monodisperse Gold Nanoparticles*, Annual Symposium of the Catalysis Society of Metropolitan New York, Princeton University, Princeton, NJ, 2019.

4. Podkolzin, S. G. In *Hydrogen Peroxide Decomposition over Mono-disperse Spectroscopically Clean Gold Nanoparticles,* 26th North American Catalysis Society Meeting (NAM26), Chicago, IL, 2019.

5. Z. Tang; Podkolzin, S. G. In *Identification of Oxygen Species on Silver Catalysts with Raman Spectroscopy and DFT Calculations,* Annual Symposium of the Catalysis Society of Metropolitan New York, New Jersey Institute of Technology, Newark, NJ, 2020 (Postponed).

6. Tang, Z.; Chen, T.; Liu, K.; Du, H.; Podkolzin, S. G., Atomic, Molecular and Hybrid Oxygen Structures on Silver; *Langmuir* **2021**, *37* (39), 11603-11610.

7. Tang, Z.; Podkolzin, S. G. In *Identification of Catalytically Active Oxygen Structures on Silver, Presentation ID 27289*, 27th North American Catalysis Society Meeting(NAM27), New York, New York, 2022.

8. Zheng, Y.; Qi, Y.; Tang, Z.; Tan, J.; Podkolzin, S. G.; Koel, B. E., Spectroscopic Observation and Structure-Insensitivity of Hydroxyls on Gold; *Journal of the American Chemical Society* **2021**, *submitted manuscript ja-2021-12980q*.

9. Qi, Y.; Zheng, Y.; Koel, B. E.; Podkolzin, S. G. In *Observation and Structure-Insensitivity of Hydroxyls on Gold, Presentation ID 27602*, 27th North American Catalysis Society Meeting(NAM27), New York, New York, 2022.

10. Zheng, Y.; Qi, Y.; Gilman, A.; Koel, B. E.; Podkolzin, S. G. In *Selective Oxidation of Ethanol over Au/ZSM-5 Catalysts,* Annual Symposium of the Catalysis Society of Metropolitan New York, Online, 2021.

11. Zheng, Y.; Qi, Y.; Gilman, A.; Koel, B. E.; Podkolzin, S. G. In *Selective Oxidation of Ethanol over Au/ZSM-5 Catalysts*, 2021 National Spring Meeting of the American Chemical Society (ACS), Online, 2021.

12. Zheng, Y.; Qi, Y.; Tan, J.; Koel, B. E.; Podkolzin, S. G. In *Selective Oxidation of Ethanol over Zeolite-Supported Gold Catalysts, Presentation ID 696533*, 27th North American Catalysis Society Meeting (NAM27), New York, New York, 2022.

13. Zheng, Y.; Tang, Z.; Podkolzin, S. G., Catalytic Platinum Nanoparticles Decorated with Subnanometer Molybdenum Clusters for Biomass Processing. *Chemistry – A European Journal* **2020**, *26* (23), 5174-5179.

14. Podkolzin, S. G.; Zheng, Y.; Tang, Z. In *Catalytic Platinum Nanoparticles Decorated with Subnanometer Molybdenum Clusters for Biomass Processing*, Science in the Age of Experience Conference 2020.

15. Zheng, Y.; Qi, Y.; Tang, Z.; Hanke, F.; Milman, V.; Podkolzin, S. G., Kinetics and Reaction Mechanisms of Acetic Acid Hydrodeoxygenation over Pt and Pt-Mo Catalysts; *ACS Sustainable Chemistry & Engineering* **2021**, *submitted manuscript sc-2021-07639c*.

16. Hofman, M. S.; Scoullos, E. V.; Robbins, J. P.; Ezeonu, L.; Potapenko, D. V.; Yang, X.; Podkolzin, S. G.; Koel, B. E., Acetic Acid Adsorption and Reactions on Ni(110); *Langmuir* **2020**, *36* (30), 8705-8715.

17. Ezeonu, L.; Robbins, J. P.; X. Yang; D.V. Potapenko; B.E. Koel; Podkolzin, S. G. In *Acetic Acid Adsorption and Reactions on Pt and Ni*, Annual Symposium of the Catalysis Society of Metropolitan New York 2020 (Postponed).

18. Ezeonu, L.; Robbins, J. P.; Tang, Z.; Yang, X.; Koel, B. E.; Podkolzin, S. G. In *Acetic Acid Adsorption and Reactions on Pt and Ni, Presentation ID 28396*, 27th North American Catalysis Society Meeting, New York, New York, 2022.

19. Y. Qi; F. Huo; E.V. Scoullos; Y. Zheng; Z. Tang; B.E. Koel; Podkolzin, S. G. In *Furfural Adsorption on Pt*, Annual Symposium of the Catalysis Society of Metropolitan New York 2020 (Postponed).

20. Huo, F.; Qi, Y.; Scoullos, E. V.; Zheng, Y.; Tang, Z.; Koel, B. E.; Podkolzin, S. G. In *Furfural Adsorption and Reactivity on Platinum Catalysts, Presentation ID 27587*, 27th North American Catalysis Society Meeting, New York, New York, 2022.

21. Robbins, J.P.; Ezeonu, L.; Yang X.; Potapenko, D. V.; Koel, B. E.; Podkolzin, S. G. In *Propylene Adsorption on Ni and Ni-Sn Catalysts*, Annual Symposium of the Catalysis Society of Metropolitan New York 2020 (Postponed).

22. Robbins, J. P.; Ezeonu, L.; Tang, Z.; Yang, X.; Podkolzin, S. G.; Koel, B. E., Propane Dehydrogenation to Propylene and Propylene Adsorption on Ni and Ni-Sn Catalysts; *ChemCatChem* **2021**, *submitted manuscript cctc.202101546R1*.

23. Robbins, J. P.; Ezeonu, L.; Tang, Z.; Yang, X.; Koel, B. E.; Podkolzin, S. G. In *Propane Dehydrogenation to Propylene on Ni and Ni-Sn Catalysts, Presentation ID 28324*, 27th North American Catalysis Society Meeting, New York, New York, 2022.

24. Podkolzin, S. G. Combining Quantum Chemical Calculations with Vibrational Spectroscopies for Studies of Reaction Mechanisms on Catalytic Surfaces. In *Invited presentation, Science Webinar by BIOVIA Corporation* Cambridge, UK, 2021.

25. Podkolzin, S. G. Catalytic Nanoparticles for Green Chemistry and Sustainability. In *Invited presentation, American Honor Society for Chemical Engineering Students, Omega Chi Epsilon, at Stevens Institute of Technology* Online, 2021.

26. Podkolzin, S. G. Supply Chain Resiliency: Synthesis of Critical Chemicals. In *Invited presentation, Department of Defense, Picatinny Arsenal* Online, 2021.

27. Zheng, Y.; Tang, Z.; Purdy, S. C.; Miller, J. T.; Podkolzin, S. G. In *Pt-Mo Catalysts for Acetic Acid Hydrodeoxygenation*, 26th North American Catalysis Society Meeting (NAM26), Chicago, IL, 2019.